Available online at www.sciencedirect.com
ScienceDirect
Phytochemistry 68 (2007) 2152–2162
PHYTOCHEMISTRY
www.elsevier.com/locate/phytochem

Measuring *in vivo* elasticities of Calvin cycle enzymes: Network structure and patterns of modulations

Michael Kreim, Christoph Giersch *

Institut für Botanik, Darmstadt University of Technology, Schnittspahnstr. 3-5, 64287 Darmstadt, Germany

Received 12 January 2007; received in revised form 28 March 2007
Available online 30 May 2007

Abstract

To measure the kinetics of enzymes, the proteins are usually assayed *in vitro* after isolation from their parent organisms. We make an attempt to show how one might determine enzyme elasticities in an intact system by a multiple modulation approach. Certain target enzymes are modulated in their activities and the changes in metabolite concentrations and flux rates upon the modulations are used to calculate the enzyme elasticities. Central to this approach is that the modulations must be independent of each other, and an algorithm is developed for finding all independent modulations that allow determining the elasticities of a given enzyme. This approach is applied to a mass-action model of the Calvin cycle. The goal is to determine the elasticities of as many enzymes as possible by modulating the activities of as few of them as possible. It is shown that the elasticities of 20 (out of 22) Calvin cycle enzymes can be determined by modulating just five reactions. Moreover, visualization of independence of modulations may be used to decompose the Calvin cycle into several sections that are independent of each other regarding flow of matter and information.

Keywords: Calvin cycle; Enzyme kinetics; Elasticity; Metabolic control analysis; Multiple modulation

1. Introduction

Enzyme kinetics is essential for understanding the dynamics and regulation of metabolic networks. Determining the kinetics of individual enzymes by the classical *in vitro* method is time-consuming and expensive in terms of labour input, and high-throughput methods are only just beginning to emerge (Gibon et al., 2004). This may be one of the reasons why classical enzyme kinetics is not popular nowadays but an endangered discipline. Another reason for the lack of popularity of enzyme kinetics has to do with its questionable relevance for the *in vivo* situation. Kinetics is done on individual enzymes that are, by biochemical methods, isolated from the parent organism and it is not clear to which degree kinetic data collected from isolated enzymes reflect their *in situ* behaviour (Fell, 1997). This is known for decades, and experimental conditions (pH, buffers, ions, etc.) are frequently given together with the kinetic data (e.g., Barman, 1974) to allow assessment to which extent the conditions are comparable. More recently, data on isolated enzymes and metabolites are compiled in electronic libraries, accessible by data mining and other bioinformatics tools (Zhang et al., 2005). However, useful as such libraries are, they are presently in some respect not much more than an electronic version of what had been published earlier in print.

Over the past decades, there have been attempts to study the role of individual enzymes for the metabolic pathway they belong to. Such attempts led to, e. g., bottleneck, rate-limiting enzyme, crossover point as essential principles of regulation (see Fell, 1997, for a summary). More recently, with the advent of high-throughput methods, other aspects of metabolic networks like topological scaling properties (Jejong et al., 2000) or correlations among metabolites (Weckwerth, 2003) attracted interest, and it seems that attempts capable of grasping certain facettes

* Corresponding author. Tel.: +49 (0) 6151 164024; fax: +49 (0) 6151 164630.
E-mail address: giersch@bio.tu-darmstadt.de (C. Giersch).

0031-9422/$ - see front matter © 2007 Elsevier Ltd. All rights reserved.
doi:10.1016/j.phytochem.2007.03.043

of the "systems" aspect of the metabolic pathway do so at the expense of quantifying its components. In this contribution, we make an attempt to use the best of both the systems and the isolated enzyme worlds by proposing how to quantify *in vivo* enzyme kinetics for all reactions of a metabolic system. We generalize an established strategy that allows one to derive information on the kinetics of individual enzymes from comparing metabolite levels and flux rates for slightly different steady states of the pathway (Kacser and Burns, 1979). The problem here is to trace the measured changes in metabolite levels and flux rates back to the level of the kinetics of individual enzymes. The main advantage of this method is that it does not require isolation of the enzymes. This method gives information that is closer to *in vivo* conditions but less quantitative than a set of kinetic data measured on an isolated enzyme.

This approach has its origin in metabolic control analysis (Kacser and Burns, 1973; Heinrich and Rappoport, 1974), but it never became a routine method for a number of reasons. One of them may be that the approach does not yield the reaction rate $v(x)$ itself but the elasticity $\partial v/\partial x$, the derivative of v with respect to metabolite concentration x. Another reason is that it requires metabolite and flux data for neighbouring steady states that are not easy to measure with sufficient accuracy (Giersch, 1995). Motivated by the increasing sensitivity and versatility of high-throughput methods for determining metabolite levels (Fiehn, 2002; Weckwerth et al., 2004; Rhee et al., 2006), we have generalized the multiple modulation approach so that it can be applied to larger pathways. We give recipes for finding proper modulations to determine *in vivo* elasticities of individual reactions of the Calvin photosynthesis cycle, and how to minimize the experimental effort. The recipes are visualized as coloured matrices. For a given enzyme, this visualization can be regarded as a map of the enzyme's role in the metabolic pathway. Both the topological structure (via the stoichiometry matrix **N**) and the mass-action and signalling structure (via the elasticity matrix **E**) contribute to this map. From compiling the maps for several individual reactions, a map for the whole metabolic system may be constructed. Thus, the recipes do not only provide information on which reactions to modulate for determining a certain elasticity. They also visualize the dependences of reactions within the metabolic pathway, thereby revealing properties of the metabolic pathway itself.

Kacser and Burns (1979) suggested double modulations for measuring elasticities in a metabolic chain without regulatory loops. In the absence of regulatory loops, v_k depends only on the concentrations of its substrate S and product P [$v_k = v_k(S,P)$]. To estimate the elasticity of reaction v_k, the first and the last reactions are modulated in their activities. From this pair of modulations it is calculated how v_k changes with S and P, so that elasticities $\partial v_k/\partial S$ and $\partial v_k/\partial P$ can be determined. The modulations are brought about by effectors p_0 and p_e that specifically modulate the activities of the first and the last reaction, respectively. The method requires the unmodulated metabolic system to be in a quasi-steady state and the modulations to lead to new quasi-steady states in the neighbourhood of the unmodulated one. The calculated elasticities $\partial v_k/\partial S$, $\partial v_k/\partial P$ are usually assumed to be valid in some neighbourhood of the unmodulated steady state.

The method has been extended to chains with feedback loops and branch points (Cornish-Bowden and Hofmeyr, 1994; Giersch and Cornish-Bowden, 1996; Elsner and Giersch, 1998). The problem with such extensions is to identify which reactions are to be modulated to determine the elasticity of a given reaction. This depends in a non-trivial way on the topology of the metabolic network, given by the stoichiometry matrix **N**, and on the network signalling structure, given by the structure (positions of non-zero entries) of its elasticity matrix **E**. The number of modulations required for determining the elasticity of a reaction is the same as the number of metabolites that affect that reaction rate. For the present work, this number is between 2 and 7, and these modulations can be dependent or independent of each other. Dependent modulations produce "parallel" changes (Elsner and Giersch, 1998) and do, therefore, not allow calculation of the elasticities. In technical terms, dependent modulations correspond to vanishing n-minors of matrix $\mathbf{A} = (\mathbf{N}\,\mathbf{E}^{\mathrm{T}})^{-1}\mathbf{N}$, where a n-minor of **A** is the determinate of a $n \times n$ submatrix of **A**. The dependence/independence information is essential for designing experiments to determine the *in vivo* elasticities of individual enzymes by means of multiple modulations. A list of reactions whose modulations allow determination of the elasticity of a given enzyme v_k is denoted as "combinatorial rule" for v_k and the combinatorial rules are visualized by means of different colours for independent sub-regions of matrix **A**. An outline of the calculation of *in vivo* elasticities is given in Appendix 1.

2. Results and discussion

2.1. Chain and cycle: elasticities for two generic pathways

Fig. 1a depicts a simple chain (9 reactions, and 8 metabolites) with pure mass-action kinetics: except at the ends, v_i is affected only by its substrate x_{i-1} and its product x_i. Reaction rate v_1 depends only on its product x_1 and v_9 only on its substrate x_8, since the concentrations of x_0 and x_e are clamped. The elasticities of reactions of the chain can be determined by double modulation. Fig. 1b visualizes, for each of the reactions 2–8, the pairs of independent modulations in different grey levels/colours. To determine the elasticity of, say, reaction 5, one of the two modulations should operate on any of the reactions 1–4 (dark grey) and the other one on any of reactions 6–9 (light grey). Fig. 1b visualizes the combinatorial rules for finding combinations of reactions whose modulations allows the determination of elasticities and the bottom line is that the elasticity of any of reactions 2–8 can be obtained by

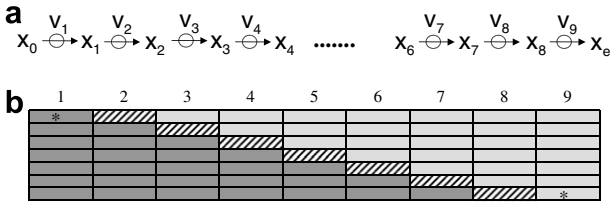

Fig. 1. (a) Simple metabolic chain with mass-action kinetics. The reaction rate v_i depends on the concentrations of its substrate x_{i-1} and product x_i: $v_i(x_{i-1}, x_i)$, $i = 2,\ldots,8$. The rates at the ends (v_1, v_9) depend on one metabolite only. (b) Combinatorial rules for the double modulation method. The rows of the scheme visualize the combinatorial rules for reactions 2,...,8, the columns represent the reactions that must be modulated. For reaction n, indicated by ▨ in column n, the two reactions to be modulated is any combination of a dark grey and light grey field in the corresponding row. To determine the elasticity of, e.g., reaction 4, one of the enzymes that must be modulated is 1 or 2 or 3, the other one is one of 5,...,9. The scheme can be summarized as indicating that one of the modulated reactions has to be upstream and one downstream of the reaction whose elasticity is to be determined. The meaning of the asterisks (*) is given in the text further below.

modulating one reaction upstream and one downstream of the reaction in question (elasticities at the ends, reaction 1 and reaction 9, can be calculated from modulating any reaction except 1 and 9, respectively). It should be noted that Fig. 1b visualizes also *all* possible modulations for any of the reactions 2–8, thus no additional pair of modulations exists for determining elasticities. Fig. 1b is a visualization of the double modulation scheme (see Kacser and Burns, 1979; Giersch and Cornish-Bowden, 1996) and is given here as an illustration for visualizing the combinatorial rules.

Fig. 2a shows a metabolic cycle (10 reactions, 8 metabolites). We assume again mass-action kinetics for all reactions so that all rates (except v_1 and v_{10}) depend on two metabolites and two modulations are sufficient to determine the elasticities. Note that this cycle is not constrained and thus distinct from a moiety-conserved cycle (Hofmeyr et al., 1986). It is only the topology of the cycle (or loop) that is of interest here. Fig. 2b visualizes the combinatorial rules for reactions 2–9. Because of the assumed mass-action kinetics, also for the cycle of Fig. 2a two modulations are sufficient in any case (only two colours are needed in Fig. 2b). However, visualization of the combinatorial rules now requires generally three or four rows, while one row was sufficient for the simple chain. The positions of reactions to be modulated cannot be arranged as "one upstream, one downstream" of the reaction of interest as for the simple chain. The total numbers of pairs of two reactions, whose modulation allows determination of the elasticities, is higher, and the combinatorial rules are less simple to summarize than for the simple chain of Fig. 1a. It is obvious, however, that four regions emerge from the changes in colours in the visualization in Fig. 2b (the regions can also be seen in Fig. 2c which is addressed further below). The regions in Fig. 2b correspond to different parts of the cycle (Fig. 2a), namely: input (reaction 1),

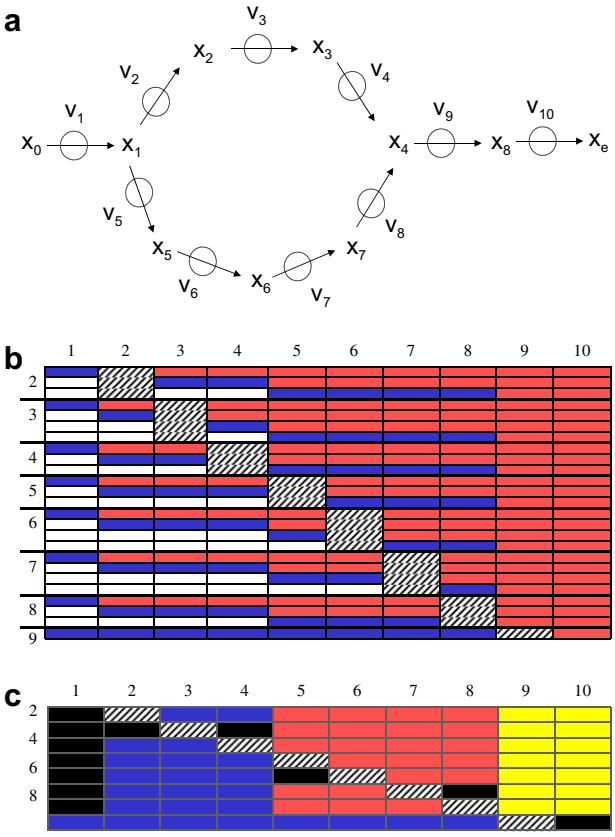

Fig. 2. (a) Simple unconstrained cycle with mass-action kinetics. The upper and lower branches, beginning with v_2 and v_5, respectively, merge at metabolite x_4. (b) Combinatorial rules for reactions 2,...,9. The meaning of the hatched field ▨ and of the colours is as for Fig. 1b. White fields do not belong to any combination. For reactions 2–8, the combinatorial rules cannot be visualized in one row (as for the simple chain of Fig. 1) but need three or four rows. For these reactions, the total number of combinations is higher than for the simple chain of comparable length. For example, there are 28 combinations of modulations to determine the qualitative kinetics of reaction 4 while this figure is 15 for reaction 4 of the simple chain. (c) Visualization of vanishing 2-minors for the simple cycle. A row number indicates the reaction whose elasticity is to be determined. All combinations of two fields of different colours in row n are pairs of independent modulations that allow one to determine the elasticity of reaction n. Black fields can be combined with any colour including black. See text further down for the significance of visualizing vanishing minors.

upper branch (2–4), lower branch (5–8), and output (9, 10). All reactions localized to one of the regions are equivalent regarding the effect on the rest of the pathway of modulating their activities and can thus substitute for each other. In hindsight, the four regions may be inferred as being equivalent from inspection of the pathway itself (Fig. 2a). Apparently, the combinatorial rules generate not only lists of independent modulations but may also be used to produce information regarding the pathway topology itself.

2.2. Combinatorial rules for the Calvin cycle

The Calvin cycle operates in the stroma of chloroplasts. It is the principal pathway of CO_2 acquisition in plants.

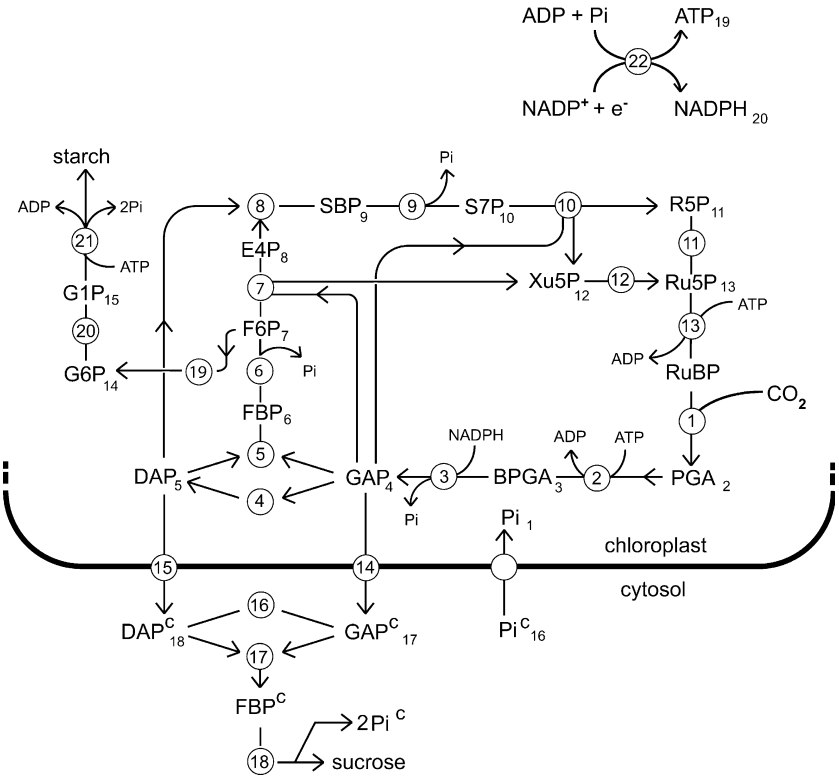

Fig. 3. Model of the Calvin cycle. The cycle operates between the "substrates" CO_2 and light and the "products" sucrose and starch, all considered to be maintained at constant levels. Most reactions of the scheme are localized to the chloroplast (upper part of the scheme) but sucrose synthesis is localized to the cytosol. Numbers in circles denote enzymes as follows: (1) ribulose 1,5-bisphosphate carboxylase/oxygenase (RubisCO); (2) 3-phosphoglycerate kinase (PGK); (3) glyceraldehyde-3-phosphate dehydrogenase (GAPDH); (4) triose phosphate isomerase (TIM); (5) 3+3 aldolase (3+3ALD); (6) fructose-1,6-bisphosphatase (FBPase); (7) 3,6 transketolase (3,6Keto); (8) 3+4 aldolase (3+4ALD); (9) sedoheptulose-1,7-bisphosphatase (SBPase); (10) 3,7 transketolase (3,7Keto); (11) phosphopentose isomerase (PPIM); (12) phosphopentose epimerase (PPEM); (13) phosphoribulokinase (PRK); (14) transenvelope exchange of GAP (v_{TR}(GAP)); (15) transenvelope exchange of DAP (v_{TR}(DAP)); (16) triose phosphate isomerase in cytosol (TIM^C); (17) 3+3 aldolase in cytosol ($3+3ALD^C$); (18) sucrose synthesis (SuSynth); (19) glucose-6-phosphate isomerase (GPI); (20) phosphoglucomutase (PGM); (21) ADP-glucose pyrophosphorylase (AGPase); (22) NADP reduction and ATP synthesis (ATPSynth). The subscript to a metabolite gives the row number of this compound in the elasticity and stoichiometry matrices.

Fig. 3 presents a simplified model of the Calvin cycle. In addition to the cycle proper, starch synthesis in the chloroplast, and photosynthate export across the chloroplast envelope for sucrose synthesis, are also considered. The pathway as depicted in Fig. 3 has 23 reactions and 22 metabolites. Owing to constraints imposed by the antiporter-principle of the phosphate translocator (see Flügge, 1999), one of the three exchange rates across the chloroplast envelope can be expressed by the two remaining ones [$v_{TR}(Pi) = -v_{TR}(DAP) - v_{TR}(GAP)$]. Likewise, the sum of the four compounds in the cytosol is conserved so that FBP^C can be expressed by DAP^C, GAP^C and Pi^C. Due to conservation of total phosphate in the chloroplast (Pi plus organic phosphate), the concentration of one of the phosphorylated compounds (here: RuBP) can be expressed by the remaining phosphorylated metabolites and Pi. The two dependent metabolites FBP^C and RuBP, and the dependent reaction rate v_{TR}(Pi) are not included in the stoichiometry and elasticity matrices. Thus, there are 20 free metabolites and 22 independent reaction rates and the stoichiometry matrix **N** (Appendix 2) is 20×22. **N** has maximum rank and there are two independent fluxes through the pathway (the dimension of the nullspace of **N** is $22 - 20 = 2$). These two fluxes correspond to net fixation of CO_2 and cycling of DAP and GAP between the chloroplast and cytosol, respectively. The elasticity matrix (Fig. 4) is based on mass-action kinetics and no regulatory loops are considered. This is not to deny the existence and importance of regulatory loops in the Calvin cycle but an attempt to restrict this first analysis to mass action. Even without regulatory loops, the reaction rates depend on up to seven metabolites (see elasticity matrix, Fig. 4). Most of the reactions usually considered as irreversible because of their large negative free energy change have been modelled as reversible (Fig. 4). Otherwise, the sensitivity structure of the Calvin cycle would break down and several more or less independent pathway sections would emerge. This is in line with the notion by Cornish-Bowden and Cárdenas (2001) that irreversibility of a model reaction should not be taken to imply complete insensitivity to reaction products which however would emerge if we modelled all reactions with large negative free energy change as irreversible. We checked the pathway sensitivity structure by inspecting flux- and concentration-control coefficients: zero entries

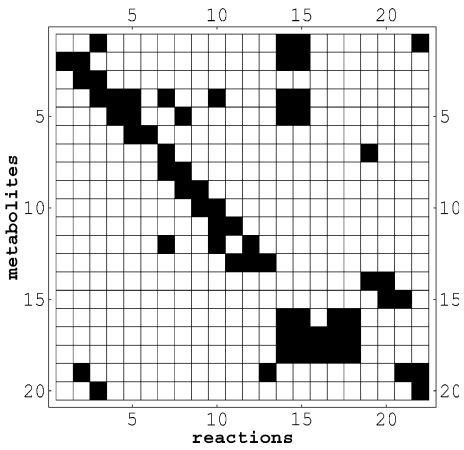

Fig. 4. Elasticity matrix **E** for the Calvin cycle model. The rows correspond to the metabolites and the columns to the reactions. See legend to Fig. 3 for denotation. A black square in the intercept of row *r* and column *c* means that the rate of reaction *c* depends on metabolite *r*. Thus reaction 5 (3+3ALD) depends on the metabolites 4 (GAP), 5 (DAP) and 6 (FBP). The rates of transenvelope exchange (columns 14 and 15) depend on all exchangeable compounds (PGA, Pi, DAP, and GAP).

in these matrices should occur only by chance and not due to zero entries in the elasticity matrix. The check was done by replacing the black squares in the elasticity matrix (Fig. 4) with random numbers.

The combinatorial rules for reactions 4 (TIM) and 9 (SBPase) are given in Fig. 5. The rates of TIM and SBPase depend on two metabolites each (see Fig. 4) so that modulations of two reactions are required in each case. For determining the elasticity of TIM (Fig. 5a), any of the "dark grey" reactions 1–18 (except TIM itself) may be chosen as one of the reactions, while the other one may be any of the "light grey" reactions in the corresponding row of Fig. 5a. If, e.g., one of the modulated reactions is PGK or GAPDH (reaction 2 or 3, second row), the other one may be any of reactions 5, 6 or 14–18 but none of reactions 7–13 or 19–22. There are altogether 131 combinations of two reactions for determining the elasticity of TIM (Table 1). For the SBPase reaction (Fig. 5b, reaction 9), one modulation can be on any of reactions 1–21 (except the SBPase reaction itself) and there are altogether 195 pairs of independent modulations. The overall pattern is somewhat different, especially regarding modulations of reactions 7–13. There are now four independent sets of these reactions (7–8, 10–11, 12, 13) while for TIM (Fig. 5a) there is only one set. This is partially due to the fact that the SBPase reaction cuts reactions 7–13 in two halves. More importantly, owing to the flux to starch (reactions 19–21), the reactions upstream and downstream of SBPase are not stoichiometrically coupled to the flux through SBPase. Another difference between Fig. 5a and b concerns the second rows: if reactions 2 or 3 are one of the modulated enzymes, determining the elasticity of TIM excludes reactions 7–13 and 19–22, while determining SBPase excludes only reaction 22. The total numbers of combinations for other reactions depending on two metabolites are of the same order as for TIM and SBPase (Table 1).

The high numbers of combinations depicted in Fig. 5 may one allow to identify two reactions whose modulations are sufficient to determine the elasticities of both reactions from only one set of modulators. Indeed, if reactions 3 and 15 are modulated, the elasticities of both TIM and SBPase can be measured (second rows of Fig. 5a and b), and there are many more combinations of two reactions that can also be employed for this purpose.

Fig. 6 shows the combinatorial rules for three reactions depending on three metabolites: PGK (reaction 2, Fig. 6a), 3+4ALD (reaction 8, Fig. 6b), and ATP synthase/NADP reduction (reaction 22, Fig. 6c). The three modulations necessary to determine the elasticities require three colours for visualization. The overall pattern of the combinatorial rules for PGK (Fig. 6a) is similar to that for TIM (Fig. 5a) with the difference that any triplet of modulations

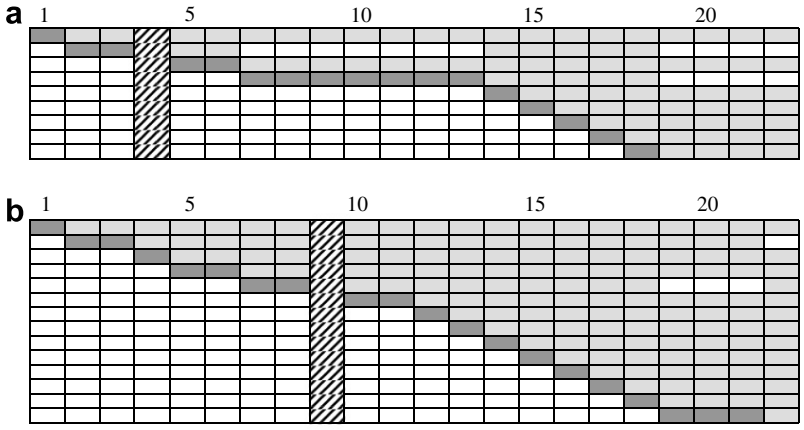

Fig. 5. (a) Pairs of independent modulations for determining the kinetics of TIM (reaction 4). The scheme visualizes the combinations of two reactions (other than TIM) that should be modulated to determine the reaction kinetics of TIM. The meaning of the hatched field (▨) and the two grey levels is as for Fig. 1b. There are altogether 131 such combinations. (b) Pairs of independent modulations for determining the kinetics of SBPase (reaction 9). There are 195 pairs of independent modulations for this reaction.

Table 1
Independent modulations for determining elasticities of Calvin cycle enzymes

Enzyme number	Enzyme name	Number of metabolites affecting rate of enzyme	Number of independent modulations	Ratio independent/total modulations
1	RubisCO	1	–	–
2	PGK	3	143	0.108
3	GAPDH	4	1134	0.189
4	TIM	2	131	0.624
5	3+3ALD	3	112	0.084
6	FBPase	1	–	–
7	3,6Keto	4	2193	0.366
8	3+4ALD	3	885	0.665
9	SBPase	2	195	0.929
10	3,7Keto	4	1260	0.211
11	PPIM	2	178	0.848
12	PPEM	2	178	0.848
13	PRK	2	170	0.810
14	v_{TR}(GAP)	7	171	0.0015
15	v_{TR}(DAP)	7	171	0.0015
16	TIM^{C}	2	131	0.624
17	3+3ALD^{C}	3	111	0.083
18	SuSynth	3	111	0.083
19	GPI	2	184	0.876
20	PGM	2	178	0.848
21	AGPase	2	170	0.810
22	ATPSynth	3	657	0.494

Total numbers of modulations are ${}_{21}C_k$ or 210, 1330, 5985 and 116,280 for $k = 2$, 3, 4 and 7 metabolites, respectively; k is the number of metabolites affecting a reaction and ${}_mC_k = m!/[k!(m-k)!]$ is the binomial coefficient.

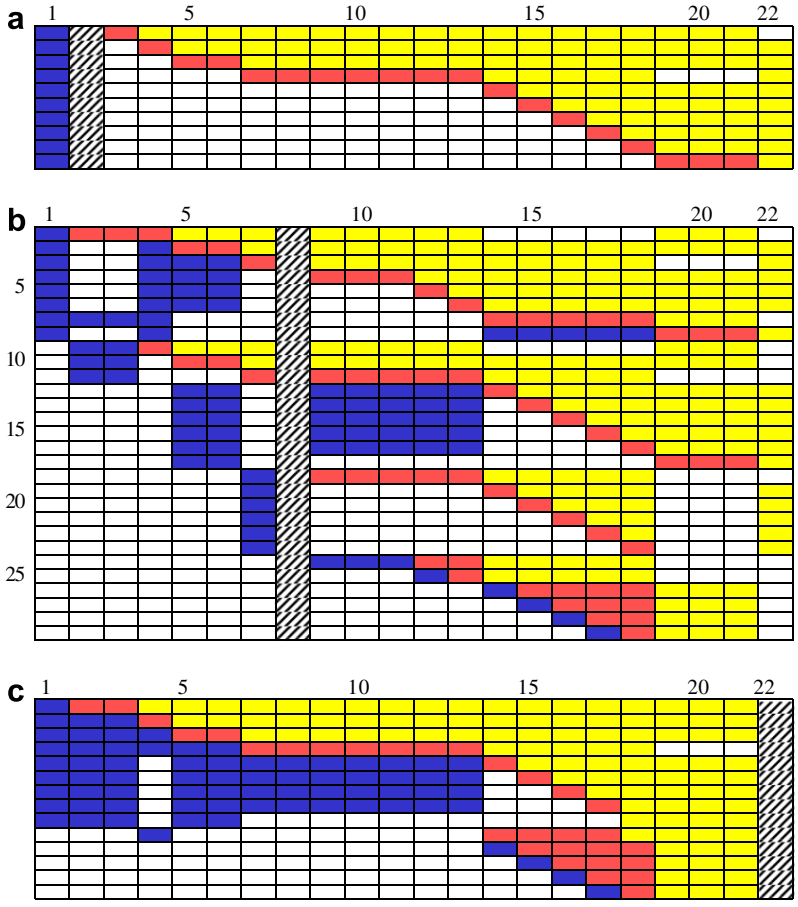

Fig. 6. Combinatorial rules for reactions depending on three metabolites. (a) PGK (reaction 2). Although now three enzymes have to be modulated, the pattern is comparable to that of the two-metabolite reactions (Fig. 5) besides that RubisCO has always to be modulated (first blue column). (b) Triplets of independent modulations for determining the elasticity of reaction 8 (3+4ALD). (c) Triplets for reaction 22 (ATPSynth).

for PGK must include the RubisCO reaction (reaction 1, Fig. 6a). So a modulator for the RubisCO reaction is indispensable if the kinetics of the PGK reaction is to be determined. For the two other reactions to be modulated there is ample choice: any of reactions 3–21 for the second reaction and almost any of reactions 3–22 as the third one. For determining the kinetics of 3+4ALD (reaction 8, Fig. 6b), the three enzymes to be modulated may be selected from almost any part of the pathway. This is due to the fact that the 3+4ALD is located at a central position in the cycle where it "sees" (is stoichiometrically coupled to) at least three segments of the Calvin cycle. Some aspects of the combinatorial rules can be understood from this intuitive type of argument: for example, if reaction 7 (6,3Keto) is the only reaction modulated in the pathway segment of reactions 1–7, the starch branch cannot contribute an independent modulation, since there is no stoichiometric coupling between the starch branch and reactions 9–22. The combinatorial rules for this choice of reactions are depicted in rows 18–24 of Fig. 6b. If however reactions 5 or 6 (or reactions 9–13) are modulated instead of reaction 7, the starch branch may well contribute to independent modulations (Fig. 6b, rows 12–17). Fig. 6c visualizes the combinatorial rules for ATPSynth and there is again a plethora of combinations for the three modulations. A major difference compared to PGK (Fig. 6a) is that almost any of reactions 1–13 may be selected if the two others are picked from reactions 14–21. The total numbers of independent modulations are 143 for PGK, 885 for 3+4ALD and 657 for the ATPSynth (Table 1).

The combinatorial rules for the other reactions of the Calvin cycle are given in their condensed form in Supplement 2 or can be generated (without condensation) from the *Mathematica* code given in Supplement 1.

2.3. Maximising the benefit of the combinatorial rules

The combinatorial rules depicted in Figs. 5, 6 and in the Supplement may be used straightaway for planning experiments to determine elasticities of Calvin cycle enzymes: from the combinatorial rules we can just look up which reactions to modulate, and then find out if the required specific effectors are available. It is obvious that there is, for any reaction, a multitude of choices for the target enzymes that are to be modulated. This allows one to consider practical and technical aspects: for which reactions are there specific inhibitors or other effectors available, for which reactions exist mutants or transgenic organisms with increased or decreased activities, and so on. Today's method of choice would be to produce cells containing antisense or RNAi constructs under the control of an inducible promoter, or *Agrobacterium*-mediated T-DNA insertional mutants (Stitt and Sonnewald, 1995; Bevan, 2002). Applying these techniques, it is feasible to reduce the expression of enzymes at certain time points during development or to completely knock down the expression of an enzyme. Production and characterisation of such constructs is very time consuming and expensive in terms of screening (which reaction(s) is/are affected), so it is desirable to construct mutants only of those reactions that are shared by the combinatorial rules for a maximum of reactions: We want to determine the elasticities of as many enzymes as possible by modulating the activities of as few enzymes as possible. That this may be rewarding is inferred from the preceding paragraph, where one pair of modulators proved sufficient to bring about the modulations necessary to determine the elasticities of both TIM and SBPase. For the reactions in the Calvin cycle model (Fig. 3), there are altogether four indispensable reactions (Supplement 2) that have to be modulated: RubisCO, required if PGK is to be determined (see also Fig. 6a), FBPase, required for 3+3ALD, sucrose synthesis, required for reaction 17 ($3{+}3ALD^{C}$), and $3{+}3ALD^{C}$, required for sucrose synthesis. From the listing of the combinatorial rules in the Supplement it can be seen that these 4 reactions (RubisCO, FBPase, $3{+}3ALD^{C}$, SuSynth) are sufficient to determine the kinetics of not less than 15 reactions of the cycle! To this figure one may add RubisCO and FBPase (each having only one entry to the elasticity matrix, Fig. 4), whose elasticities can be determined from single modulations. In fact, if PPEM (reaction 12) is included as the fifth reaction, it is feasible to determine the elasticities of 20 (out of the 22) reactions of the Calvin cycle. If, in addition, reactions 4 (TIM) and 16 (TIM^{C}) are modulated, the elasticities of all 22 reactions may be determined (Supplement 2). Thus, owing to the richness of the patterns of the combinatorial rules, five sets of gene constructs are sufficient to allow the determination of elasticities of 20 enzymes in the Calvin cycle, and seven sets for determining all of them.

For reactions depending on two metabolites, the numbers of independent pairs of combinations vary between 131 and 195 (Table 1). For reactions with three metabolites, the lowest number of independent triplets is 112 (3+3ALD) and the highest 885 (3+4ALD). We may define the *modulability* of a reaction by the ratio of independent combinations to all combinatorially feasible (independent plus dependent) ones. The latter are 210, 1330 and 5985 for reactions depending on two, three and four metabolites, respectively (calculated from the binomial coefficient $_{21}C_k = 21!/[k!(21-k)!]$ for $k = 2$, 3 or 4). The modulabilities of the Calvin cycle reactions that depend on two, three or four metabolites varies between 0.083 (reactions 17 and 18) and 0.929 for GPI (reaction 9). The translocator reactions v_{TR}(DAP) and v_{TR}(GAP) with their extremely low modulabilities are not considered here. The higher the modulability of a reaction, the greater the chance of finding an effector for this reaction. Modulators for reactions with low modulabilities (e.g., reactions 17 and 18, modulability lower than 0.1) are less likely to be available than those with high modulability. Thus, (1 – modulability) can be considered as a measure for the "cost" for finding proper modulators. The GPI reaction has the lowest cost (0.07) while reactions 17 and 18 have the highest cost (0.92),

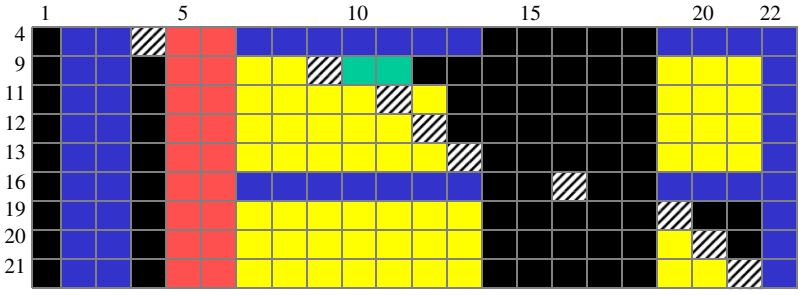

Fig. 7. Regions of vanishing 2-minors for the 8 reactions of the Calvin cycle model that depend on two metabolites. The row numbers on the left of the scheme are the enzyme numbers (Fig. 3). Colour code is as for Fig. 2c and applies to the individual rows: different sections of vanishing 2-minors are given in different colours, and the black sections represent non-vanishing 2-minors. Any combination of two different colours and any combination of a black field with another black field or a coloured field corresponds to an independent combination of modulations. See text for further details.

and one may maximise the benefit of the combinatorial rules also with respect to these costs.

It is tempting to consider the modulability of a reaction also as an indicator of the number of parts in which a pathway is fragmented when "seen" from that reaction. Modulability should then be the same for all reactions in the simple chain (Fig. 1), since the chain is fragmented in two parts for any reaction. Modulability for the simple chain, however, increases from $1 \times 7/{}_8C_2 = 7/28 = 0.25$ for the second (or second from last) reaction to $4 \times 4/{}_8C_2 = 16/28 = 0.57$ for reaction 5 in the mid of the pathway. Thus, to transform the modulability into an indicator of a network property, one would have to account for the fact that the number of combinations (that depend on the reaction's position in a chain-like pathway sections) contribute to modulability.

2.4. Regions of vanishing minors as complements of combinatorial rules

The combinatorial rules can be visualized in more condensed form: instead of listing independent combinations (as in Figs. 1, 2, 5, 6 and Supplement 2) we can start from the set of all feasible combinations of reactions and subtract the dependent ones. The set of all feasible combinations may be visualized by a row of black fields and dependent combinations are given as coloured segments in this black background. Fig. 2c shows the vanishing 2-minors for the simple cycle of Fig. 2a. All reactions that are not independent have the same colour and one has to pick two reactions with different colours to find a non-vanishing minor. A black field is not part of any vanishing 2-minor and can, therefore, be combined with any of the colours (including black) to obtain a non-vanishing 2-minor. Any two reactions are independent as long as they have different colours, and reactions marked in black are independent in any case. According to the combinatorial rules for the simple cycle, there are, to modulate reaction 2, 8 combinations (Fig. 2b, line 1) $+ 2 \times 6$ (line 2) $+ 4 \times 2$ (line 3), together 28 combinations. From Fig. 2c there is a total of ${}_9C_2 = 36$ combinations to select a pair of reactions for determining the elasticity of reaction 2, and of these combinations the following have zero minors: 1 (blue) + 6 (red) + 1 (yellow), together 8 combinations. Thus, $36 - 8 = 28$ have minors different from zero. The regions of vanishing 2-minors (Fig. 2c) present in a more condensed form the same information regarding independence of modulations as the combinatorial rules (Fig. 2b). The regions of vanishing 2-minors for the simple chain of Fig. 1a are the same as the combinatorial rules of Fig. 1b with the fields in the upper left and lower right corners turned black (marked by an asterisk (*) in Fig. 1b).

Fig. 7 depicts the vanishing 2-minors for the 9 reactions of the Calvin cycle that depend on two metabolites (see **E** matrix, Fig. 4). Two, three or four different colours are required to visualize the minors, corresponding to two, three and four independent regions of vanishing 2-minors. As before, black is to symbolise fields that do not depend on other fields and can thus be combined with any other field (including a black one) to give rise to a pair of independent modulations. The vanishing 2-minors for reaction 4 (TIM) are given in the first row. From the combinatorial rules for this reaction (Fig. 5a) it is clear that selecting reaction 2 or 3 as the first reaction excludes reactions 7–13 and 19–22. Thus reactions 2, 3, 7–13, 19–22 are one single region of vanishing 2-minors (blue fields in Fig. 7). That the fields of vanishing minors are the same for reactions 4 (TIM) and 16 (TIM^C) is related to the fact that they have the same role in different compartments and that the pathway sections to which these enzymes belong are mirror images of each other. Also reactions 5 and 17 (3+3ALD in the chloroplast and cytosol) show a high similarity regarding vanishing minors (Supplement 2) with the exception that the FBPase reaction in the chloroplast must always be modulated if the stroma 3+3ALD is to be determined. Reaction 9 (Fig. 7, row 2) requires four colours for visualization, and this is due to high numbers of combinatorial rules for this reaction (SBPase has the highest modulability, Table 1). Reactions 19–21 are the branch for starch synthesis and have similar regions of vanishing minors. For this branch, and for reactions 11–13 (Ru5P and RuBP synthesis) three different colours are required to visualize the vanishing minors.

3. Conclusion and outlook

3.1. Will the multiple modulation method work in practice?

Determining the elasticities of an enzyme requires measurement of the differences in flux rates and metabolite concentrations brought about by the modulations of enzyme activities (see above and Fell, 1997; Giersch, 1995). It is a difficult and tedious task to measure the small differences in flux rates and metabolite concentrations with the required accuracy, and this has limited so far the use of the multiple modulation approach. Recent progress in high-throughput methods (Weckwerth et al., 2004) may help to circumnavigate the problem. Presently, about 100 compounds can be measured in one run with an accuracy of about 20% standard deviation. Although this is not quite sufficient to make the determination of elasticities by multiple modulations a routine method, there is hope that this will be so in the future. Until then, a promising strategy may be not to attach numbers to the $\partial S_j/\partial p_k$ or $\partial J/\partial p_k$ but to qualify them as small/large in addition to increasing/decreasing. This type of information may be sufficient to qualify also the elasticities according to small/large, plus/minus. For small systems (up to three variables) it is conceivable that the sign or even the size of an elasticity $\partial v_i/\partial x_j$ can be calculated from such qualitative data on the $\partial S_j/\partial p_k$ and $\partial J/\partial p_k$.

3.2. Vanishing minors and pathway structure

Visualization of the vanishing minors (Figs. 2c and 7) needs less space than visualization of the combinatorial rules, since the regions of vanishing minors start from one black row representing all feasible combinations from which the dependent ones are subtracted. Structural elements of a pathway are easier to identify from the condensed vanishing-minors representation. For the simple cycle (Fig. 2c) four pathway sections were identified from the vanishing minors that correspond to four topologically different sections (see above). From Fig. 7 one may identify several sections of the Calvin cycle: four sections of at least two reactions (2–3,22), (5–6), (7–13), (19–21) are separated by individual reactions (RubisCO, reaction 1 and TIM, reaction 4) or a block (14–18) of independent reactions. The enzyme members of the coloured sections are functionally equivalent regarding their roles in twofold modulation, that is, one member of a section can be exchanged for another one of the same section. Thus it is not surprising that some of the sections can be identified with short segments of a simple chain (reactions 2–3, 5–6, starch branch 19–21). The largest section (reactions 7–13) corresponds to the regenerative segment of the Calvin cycle, and it may be surprising that the enzyme members of this highly branched section can substitute for each other (unless the elasticity of a reaction from this section is to be determined). The high number of branches (due to transketolase and aldolase) provides strict stoichiometric coupling in the section.

The most independent section is reactions 14–18 (transenvelope exchange and sucrose synthesis in the cytosol). From the nullspace of stoichiometry matrix, cycling of DAP and GAP between the chloroplast stroma and the cytosol (with DAP-GAP interconversion catalysed by the TIMs) is one of the steady-state fluxes (see above). This cycling, superimposed to net photosynthate export, decouples the stoichiometry of sucrose synthesis from the Calvin cycle proper. The reactions of the sucrose branch (reactions 14–18) are thus independent of each other, at least as "seen" by the reactions listed in Fig. 7. This, however, is only half the truth: from Fig. 6b, rows 7 and 8, it is obvious that for the 3+4ALD the reactions of the sucrose synthesis section are by no means independent of each other.

The pathway sections emerge already from visualizing the vanishing minors, provided minor differences among individual rows are ignored (Figs. 2c and 7). All information given in these figures is extracted from the matrix $\mathbf{A} = (\mathbf{N}\ \mathbf{E}^{\mathrm{T}})^{-1}\mathbf{N}$, and it may be promising to visualize the vanishing minors on matrix **A** itself. The resulting 20×22 matrix will show all 2-minors, and the rows of this matrix can be identified with the metabolites (the columns correspond to the reactions). In its final version, the suggested matrix should not only show 2-minors but also minors of higher orders. For the Calvin cycle model, such a visualization should depict the regions for 2-, 3-, 4- and 7-minors, corresponding to the numbers of metabolites that affect individual reactions. Such a matrix would contain all the available information on dependences of the Calvin cycle reactions. Fig. 7 is a sort of nucleus (or condensed preliminary sketch) of this matrix. The final version of such a matrix may serve as a map of dependences within a metabolic pathway.

It should be noted that Fig. 7 (and the suggested visualization of all vanishing minors on matrix **A**) is a *mixtum compositum* of the stoichiometric (given by the stoichiometry matrix **N**) and the signalling structure of the network (given by the elasticity matrix **E**). It maps dependences both regarding flow of matter and flow of information, the latter via mass action and regulatory loops. That only flow of matter was considered in our analysis (regulatory loops were not included in matrix **E**, Fig. 4) has mainly pragmatic reasons. Calculation of independent modulations for reactions depending on more than three metabolites is tedious and time-consuming without more elaborate software than presently available. Since any regulatory loop means an extra entry to the elasticity matrix **E**, we decided to stick to the minimum version that features only the flow of matter, but with the irreversible reactions modelled as reversible ones to avoid zero control coefficients (see above). Thus, our model is final regarding the flow of matter and of information carried by material flow. It should be noted,

however, that our approach is not limited to a mass-action **E** matrix. If, e.g., the two well-known effectors Pi and 3-PGA of reaction 21 (AGPase) are included in the analysis, the number of independent modulations for this reaction increases from 170 to 570, yet 7 modulations are still sufficient to determine all 22 elasticities as was the case for the mass-action model. The higher numbers of independent modulations (570 versus 170) obtained when regulatory loops are included in matrix **E** increase the chance of finding a proper combination of four (instead of two) modulations among the combinations already employed. We expect that the total number of required modulations is only slightly higher than 7 if all regulatory loops are considered for the Calvin cycle model.

Acknowledgement

We thank Theresa Stang for helpful mathematical discussions and Doris Schäfer and Mirja Skrablin for assistance in preparing the figures

Appendix 1. Independence of modulations

Which reactions have to be modulated to determine the elasticities of reaction v_k has been considered before in detail (Giersch and Cornish-Bowden, 1996) and can be summarized as follows. The elasticities $\partial v_k/\partial x_j$ are calculated from

$$\begin{pmatrix} \frac{\partial S_1}{\partial p_1} & \cdots & \frac{\partial S_m}{\partial p_1} \\ \vdots & & \vdots \\ \frac{\partial S_1}{\partial p_n} & \cdots & \frac{\partial S_m}{\partial p_n} \end{pmatrix} \begin{pmatrix} \frac{\partial v_1}{\partial x_1} & \cdots & \frac{\partial v_n}{\partial x_1} \\ \vdots & & \vdots \\ \frac{\partial v_1}{\partial x_m} & \cdots & \frac{\partial v_n}{\partial x_m} \end{pmatrix} = \begin{pmatrix} ? & \frac{\partial J^2}{\partial p_1} & \cdots & \frac{\partial J^{n-1}}{\partial p_1} & \frac{\partial J^n}{\partial p_1} \\ \frac{\partial J^1}{\partial p_2} & ? & \cdots & \frac{\partial J^{n-1}}{\partial p_2} & \frac{\partial J^n}{\partial p_2} \\ \vdots & \vdots & \ddots & \vdots & \vdots \\ \frac{\partial J^1}{\partial p_{n-1}} & \frac{\partial J^2}{\partial p_{n-1}} & \cdots & ? & \frac{\partial J^n}{\partial p_{n-1}} \\ \frac{\partial J^1}{\partial p_n} & \frac{\partial J^2}{\partial p_n} & \cdots & \frac{\partial J^{n-1}}{\partial p_n} & ? \end{pmatrix}, \tag{1a}$$

or in short

$$\left(\frac{\partial S}{\partial p}\right)^{\mathrm{T}} \mathbf{E} = \left[{}_{?}\left(\frac{\partial J}{\partial p}\right)_{?} \right]^{\mathrm{T}} \tag{1b}$$

The $\partial S_i/\partial p_j$ and the $\partial J^{\mathrm{r}}/\partial p_j$ are assumed to be known from experiments. They can be determined by measuring S_i and J^{r} for various concentrations of p_j to get the slope of $S_i(p_j)$ and $J^{\mathrm{r}}(p_j)$, see Giersch (1995) and Fell (1997) for details. The elasticities of v_k can be obtained by solving the linear system:

$$\begin{pmatrix} \frac{\partial S_1}{\partial p_1} & \cdots & \frac{\partial S_m}{\partial p_1} \\ \vdots & & \vdots \\ \frac{\partial S_1}{\partial p_n} & \cdots & \frac{\partial S_m}{\partial p_n} \end{pmatrix} \begin{pmatrix} \frac{\partial v_k}{\partial x_1} \\ \vdots \\ \frac{\partial v_k}{\partial x_m} \end{pmatrix} = \begin{pmatrix} \frac{\partial J^k}{\partial p_1} \\ \vdots \\ ? \\ \vdots \\ \frac{\partial J^k}{\partial p_n} \end{pmatrix} \leftarrow \text{position } k \tag{2}$$

Frequently, only some (2–4) of the m elasticities in $(\partial v_k/\partial x_1,\ldots,\partial v_k/\partial x_{\mathrm{m}})^{\mathrm{T}}$ are different from zero and it is sufficient to select only some of the rows of the matrix $(\partial \mathbf{S}/\partial \mathbf{p})^{\mathrm{T}}$ to get as many equations as there are non-zero unknowns in $(\partial v_k/\partial x_1,\ldots,\partial v_k/\partial x_{\mathrm{m}})^{\mathrm{T}}$. It is essential that the selected rows are linearly independent, or, in technical terms, that the corresponding low-order sub-matrices of the matrix $(\partial \mathbf{S}/\partial \mathbf{p})^{\mathrm{T}}$ have maximum rank so that their determinants are different from zero. Note that row k of $(\partial \mathbf{S}/\partial \mathbf{p})^{\mathrm{T}}$ cannot be used to solve Eq. (1) since there is no right-hand-side in this case. The columns of the elasticity matrix of the Calvin cycle have from 1 to 7 entries. It is computed which of the corresponding submatrices have maximum rank (= non-vanishing minor), and these are visualized. To calculate the set of non-vanishing minors for, e.g., reaction 2, we delete row 2 from $(\partial \mathbf{S}/\partial \mathbf{p})^{\mathrm{T}}$ and collect columns 2, 3 and 19 (column 2 of the elasticity matrix has non-zero entries only in theses rows) to get a matrix with 21 rows and 3 columns. The total number of 3-minors of this matrix is ${}_{21}\mathrm{C}_3 = 1330$. The non-zero minors are identified by means of the fact that $(\partial \mathbf{S}/\partial \mathbf{p})^{\mathrm{T}}$ has the same structure of non-vanishing minors as $[\mathbf{N}\ \mathbf{E}^{\mathrm{T}}]^{-1}\mathbf{N}$ (see (Giersch and Cornish-Bowden, 1996)). Which 3-minors are non-zero is calculated by means of a *Mathematica* code (Supplement 1). Based on this list, non-vanishing n-minors are then visualized using n different colours: any combination of n reactions corresponds to a non-vanishing n-minor as long as the n colours are different. Some of the combinations from the Supplement 2 are further condensed and presented in Figs. 5 and 6 as "combinatorial rules". From the combinatorial rules or their un-condensed versions the minimum sets of modulations required for determining the elasticities of as many reactions as possible are selected manually: the list of indispensable modulations is completed by appropriate additional ones which are found by trial and error. The combinatorial rules may also be visualized indirectly by giving regions of vanishing minors, the complement of the combinatorial rules (Fig. 7). The regions of vanishing minors represent the patterns of modulations in their most condensed form.

Appendix 2. Stoichiometry matrix N for the Calvin cycle model

Stoichiometry matrix **N** for the Calvin cycle model. Rows and columns refer to the same compounds and reactions, respectively, as given for the elasticity matrix **E** in Fig. 4.

$$\begin{pmatrix}
0 & 0 & 1 & 0 & 0 & 1 & 0 & 0 & 1 & 0 & 0 & 0 & 0 & 1 & 1 & 0 & 0 & 0 & 0 & 0 & 2 & -1 \\
2 & -1 & 0 & 0 & 0 & 0 & 0 & 0 & 0 & 0 & 0 & 0 & 0 & 0 & 0 & 0 & 0 & 0 & 0 & 0 & 0 & 0 \\
0 & 1 & -1 & 0 & 0 & 0 & 0 & 0 & 0 & 0 & 0 & 0 & 0 & 0 & 0 & 0 & 0 & 0 & 0 & 0 & 0 & 0 \\
0 & 0 & 1 & -1 & -1 & 0 & -1 & 0 & 0 & -1 & 0 & 0 & 0 & -1 & 0 & 0 & 0 & 0 & 0 & 0 & 0 & 0 \\
0 & 0 & 0 & 1 & -1 & 0 & 0 & -1 & 0 & 0 & 0 & 0 & 0 & 0 & -1 & 0 & 0 & 0 & 0 & 0 & 0 & 0 \\
0 & 0 & 0 & 0 & 1 & -1 & 0 & 0 & 0 & 0 & 0 & 0 & 0 & 0 & 0 & 0 & 0 & 0 & 0 & 0 & 0 & 0 \\
0 & 0 & 0 & 0 & 0 & 1 & -1 & 0 & 0 & 0 & 0 & 0 & 0 & 0 & 0 & 0 & 0 & 0 & -1 & 0 & 0 & 0 \\
0 & 0 & 0 & 0 & 0 & 0 & 1 & -1 & 0 & 0 & 0 & 0 & 0 & 0 & 0 & 0 & 0 & 0 & 0 & 0 & 0 & 0 \\
0 & 0 & 0 & 0 & 0 & 0 & 0 & 1 & -1 & 0 & 0 & 0 & 0 & 0 & 0 & 0 & 0 & 0 & 0 & 0 & 0 & 0 \\
0 & 0 & 0 & 0 & 0 & 0 & 0 & 0 & 1 & -1 & 0 & 0 & 0 & 0 & 0 & 0 & 0 & 0 & 0 & 0 & 0 & 0 \\
0 & 0 & 0 & 0 & 0 & 0 & 0 & 0 & 0 & 1 & -1 & 0 & 0 & 0 & 0 & 0 & 0 & 0 & 0 & 0 & 0 & 0 \\
0 & 0 & 0 & 0 & 0 & 0 & 1 & 0 & 0 & 1 & 0 & -1 & 0 & 0 & 0 & 0 & 0 & 0 & 0 & 0 & 0 & 0 \\
0 & 0 & 0 & 0 & 0 & 0 & 0 & 0 & 0 & 0 & 1 & 1 & -1 & 0 & 0 & 0 & 0 & 0 & 0 & 0 & 0 & 0 \\
0 & 0 & 0 & 0 & 0 & 0 & 0 & 0 & 0 & 0 & 0 & 0 & 0 & 0 & 0 & 0 & 1 & 0 & 1 & -1 & 0 & 0 \\
0 & 0 & 0 & 0 & 0 & 0 & 0 & 0 & 0 & 0 & 0 & 0 & 0 & 0 & 0 & 0 & 0 & 0 & 0 & 1 & -1 & 0 \\
0 & 0 & 0 & 0 & 0 & 0 & 0 & 0 & 0 & 0 & 0 & 0 & 0 & -1 & -1 & 0 & 0 & 2 & 0 & 0 & 0 & 0 \\
0 & 0 & 0 & 0 & 0 & 0 & 0 & 0 & 0 & 0 & 0 & 0 & 0 & 1 & 0 & -1 & -1 & 0 & 0 & 0 & 0 & 0 \\
0 & 0 & 0 & 0 & 0 & 0 & 0 & 0 & 0 & 0 & 0 & 0 & 0 & 0 & 1 & 1 & -1 & 0 & 0 & 0 & 0 & 0 \\
0 & -1 & 0 & 0 & 0 & 0 & 0 & 0 & 0 & 0 & 0 & 0 & -1 & 0 & 0 & 0 & 0 & 0 & 0 & 0 & -1 & 1 \\
0 & 0 & -1 & 0 & 0 & 0 & 0 & 0 & 0 & 0 & 0 & 0 & 0 & 0 & 0 & 0 & 0 & 0 & 0 & 0 & 0 & \frac{8}{9}
\end{pmatrix}$$

Appendix 3. Supplementary material

Supplementary data associated with this article can be found, in the online version, at doi:10.1016/j.phytochem.2007.03.043.

References

Barman, T.E., 1974. Enzyme Handbook. Springer, New York.

Bevan, M., 2002. Genomics and plant cells: application of genomic strategies to *Arabidopsis* cell biology. Phil. Trans. R. Soc. Lond. B 357, 731–736.

Cornish-Bowden, A., Cárdenas, M.L., 2001. Information transfer in metabolic pathways. Effects of irreversible steps in pathway models. Eur. J. Biochem. 268, 6616–6624.

Cornish-Bowden, A., Hofmeyr, J.-H.S., 1994. Determination of control coefficients in intact metabolic systems. Biochem. J. 298, 367–375.

Elsner, L., Giersch, C., 1998. Metabolic control analysis: separable matrices and interdependence of control coefficients. J. Theor. Biol. 193, 649–661.

Fell, D., 1997. Understanding the Control of Metabolism. Portland Press, London.

Fiehn, O., 2002. Metabolomics – the link between genotypes and phenotypes. Plant Mol. Biol. 48, 155–171.

Flügge, U.I., 1999. Phosphate translocators in plastids. Ann. Rev. Plant Physiol. Plant Mol. Biol. 50, 27–45.

Gibon, Y., Blaesing, O.E., Hannemann, J., Carillo, P., Höhne, M., Hendriks, J.H.M., Palacios, N., Cross, J., Selbig, J., Stitt, M., 2004. A robot-based platform to measure multiple enzyme activities in *Arabidopsis* using a set of cycling assays: comparison of changes of enzyme activities and transcript levels during diurnal cycles and in prolonged darkness. Plant Cell 16, 3304–3325.

Giersch, C., 1995. Determining elasticities from multiple measurements of flux rates and metabolite concentrations: application of the multiple modulation method to a reconstituted pathway. Eur. J. Biochem. 227, 194–201.

Giersch, C., Cornish-Bowden, A., 1996. Extending double modulation: combinatorial rules for identifying the modulations necessary for determining elasticities in metabolic pathways. J. Theor. Biol. 182, 361–369.

Heinrich, R., Rappoport, T.A., 1974. A linear steady-state treatment of enzymatic chains: general properties, control and effector strength. Eur. J. Biochem. 42, 89–95.

Hofmeyr, J.-H.S., Kacser, H., van der Merwe, K.J., 1986. Metabolic control analysis of moiety-conserved cycles. Eur. J. Biochem. 155, 631–641.

Jejong, H., Tombor, B., Albert, R., Ottavi, Z.N., Barabási, A.-L., 2000. The large-scale organization of metabolic networks. Nature 407, 651–654.

Rhee, S.Y., Dickerson, J., Xu, D., 2006. Bioinformatics and its applications in plant biology. Ann. Rev. Plant Biol. 57, 335–360.

Stitt, M., Sonnewald, U., 1995. Regulation of metabolism in transgenic plants. Ann. Rev. Plant Physiol. Plant Mol. Biol. 46, 341–368.

Kacser, H., Burns, J.A., 1973. The control of flux. Symp. Soc. Exp. Biol. 27, 65–104.

Kacser, H., Burns, J.A., 1979. Molecular democracy: who shares the controls? Biochem. Soc. Trans. 7, 1149–1160.

Zhang, P., Foerster, H., Tissier, C.P., Mueller, L.A., Paley, S., Karp, P.D., Rhee, S.Y., 2005. MetaCyc and AraCyc: metabolic pathway databases for plant research. Plant Physiol. 138, 27–37.

Weckwerth, W., 2003. Metabolomics in systems biology. Ann. Rev. Plant Biol. 54, 669–689.

Weckwerth, W., Loureiro, M., Wenzel, K., Fiehn, O., 2004. Differential metabolic networks unravel the effects of silent plant phenotypes. Proc. Natl. Acad. Sci. USA 101, 7809–7814.